CHAPTER 5

MODELLING AND OPTIMIZATION OF EROSION PARAMETERS USING RSM AND ANN

5.1 INTRODUCTION

The erosion is dependent on several factors and to study the effect of each factor in combination with other factors will leads to several undesirable experimentations. Statistical modelling is a tool which helps to eradicate the redundancy during experimentation and also to optimize the basic objective function. Studying the effect of these variables, there is an enormous scope of implementing statistical techniques for analysis, prediction, and optimization to obtain the maximum benefit. The present investigation addresses this aspect by using Response Surface Methodology (RSM). RSM is a multivariate technique based on the fit of a polynomial equation to statistical data, with an objective to simultaneously optimize the levels of these variables to attain the best system performance. To approximate a response function to experimental data, a quadratic response surface, i.e., Central Composite Rotatable Design (CCRD) is used in the present study.

Artificial neural network (ANN) offers an alternative to the polynomial regression method as a modelling tool. Advances in computing power have enabled the application of ANN in providing non-linear modelling for response surfaces and optimization. McCulloch and Pitts [164] developed an ANN model based on their knowledge of neurology. Paul Werbos [165] contribution to the back-propagation learning method is recognized as the most significant contribution. Velten et al. [166] and Zhang et al. [167] were among the first to implement ANN to analyze the wear of polymer composites. Palavar et al. [168] used ANN to predict the wear behaviour of IN706 superalloy. To predict the wear behaviour of aluminium alloys and its composites, ANN has been widely used [169–171]. More recently work by Suresh et al. [172] reports successful implementation of ANN in predicting solid particle erosion in composites. A multilayer feed-forward network with a back-propagation training algorithm has been used widely in wear prediction [167]. Hence, artificial neural networks (ANNs) have been extensively used for the prediction of wear data in tribological tests [173]. In view of the above, erosion tests is conducted to evaluate the high-temperature steady-state erosion rate of Type 446 SS at the higher temperature and the parameters responsible for minimum loss of material under erosion is optimized with the help of RSM and ANN technique.

5.2 RESULTS AND DISCUSSION

The digital photograph of the eroded scar surface is shown in Fig.5.1. It is seen that the appearance on the tested surface differs with test conditions due to the formation of an oxide layer on the surface when exposed to high temperatures. These oxides are also considered to act as a protective layer, thereby, prevents the direct contact of abrasives with the material surface. Further, worn surfaces were examined using a scanning electron microscope (FEI Nova NanoSEM450) to determine the possible erosion mechanism.

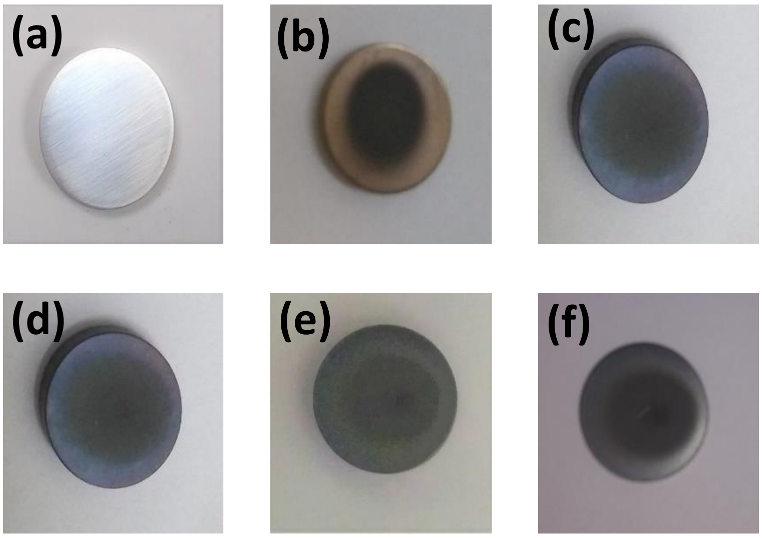

Fig.5.1: Macrograph of **(a)** un-eroded and **(b-f)** eroded surface under test temperature of 350°C, 450°C, 550°C, 650°C and 750°C respectively.

5.2.1 Central composite rotatable design (CCRD)

CCRD presented by Box and Wilson [174] is most widely preferred for the second-order response surface model as they are relatively efficient concerning the number of runs required. The second-order model is usually required to approximate the curvature in the true response surface when the experimenter is close to optimum [175].

The fitted second-order response surface model is given by equation (5.1):

$$\eta = \beta_o + \sum_{i=1}^{k} \beta_i x_i + \sum_{i=1}^{k} \beta_{ii} x_i^2 + \sum \sum_{i<j=2}^{k} \beta_{ij} x_i x_j \qquad (5.1)$$

Where η is response; x_i $(1, 2, \ldots k)$ is the coded level of k quantitative variables; β_o is the constant term, and β_i, β_{ii} and β_{ij} are the coefficients of the linear expansion.

Full uniformly routable central composite design presents the following characteristics:

a) Requires an experiment number according to N = $k^2 + 2k + C_p$, where k is the factorial number and (C_p) is the replicate number of the central point.

b) α- value depends on the number of variables and can be calculated as $\alpha = 2^{(k-p)/4}$.

In the present investigation, its value is 1.682

c) all factors are studied in five levels (-α, -1, 0, +1, +α).

Table 5.1 presents the process parameters at five different levels, and Table 5.2 shows the design matrix of twenty iterations, according to the CCRD technique, to calculate the erosion rate of the sample. To analyze the regression model, a software package of MINITAB 18 has been used.

Table 5.1: Erosion parameters and their levels.

Parameters	Notation	Units	Levels				
			-1.682	-1	0	1	1.682
Test temperature	A	°C	350	450	550	650	750
Impact velocity	B	m/s	40	55	70	85	100
Impact angles	C	Degree	30	45	60	75	90

5.2.2 Analysis of variance (ANOVA) and regression model for Erosion rate

The regression coefficients evaluated using ANOVA have significantly determined each factor regarding erosion rate as shown in Table 5.3. The model for erosion rate employing R^2 = 94.54% signifies that the model is compatible with total variance at 95% confidence limit. P-values less than 0.05 reveal that the model is statically significant for optimization.

Table 5.2: Experimental results for Erosive Wear of Type 446 stainless steel.

Experimental Run	Erosion Parameters			Erosion Rate (gm/gm x10^{-5})
	A	B	C	
1	550	70	60	10.151
2	550	70	60	10.158
3	750	70	60	15.463
4	450	85	45	10.395
5	550	70	30	11.269
6	650	55	75	12.539
7	350	70	60	7.936
8	550	70	60	10.148
9	550	100	60	18.095
10	650	85	75	14.503
11	550	40	60	9.523
12	550	70	90	8.573
13	450	55	45	6.140
14	550	70	60	10.143
15	550	70	60	10.156
16	450	55	75	5.654
17	550	70	60	10.139
18	450	85	75	8.746
19	650	55	45	14.601
20	650	85	45	16.269

Table 5.3: Analysis of variance for Erosion rate.

Source	DF	Adj SS	Adj MS	F-Value	P-Value
Model	9	193.938	21.549	19.25	0.000
Linear	3	170.326	56.775	50.73	0.000
Test temperature	1	115.034	115.034	102.78	0.000
Impact velocity	1	47.223	47.223	42.19	0.000
Impact angles	1	8.068	8.068	7.21	0.023
Square	3	21.435	7.145	6.38	0.011
2-Way Interaction	3	2.177	0.726	0.65	0.602
Error	10	11.192	1.119		
Lack-of-Fit	5	11.192	2.238	41323.96	0.000
Pure Error	5	0.000	0.000		
Total	19	205.130			

Response surface regression equation is obtained as:

$$\text{Erosion rate} = 10.175 + 2.902\,A + 1.860\,B - 0.769\,C + 0.378\,A*A + 1.224\,B*B$$

$$- 0.250\,C*C - 0.464\,A*B - 0.212\,A*C - 0.108\,B*C$$

$$R^2 = 94.54\%$$

Normal probability plot shown in Fig. 5.2 confirms that all the residues are falling on a straight line with errors being positioned normally and no scattering is observed. The percentage contribution of each parameter measures tests temperature as the most influencing parameter with 56.07%.

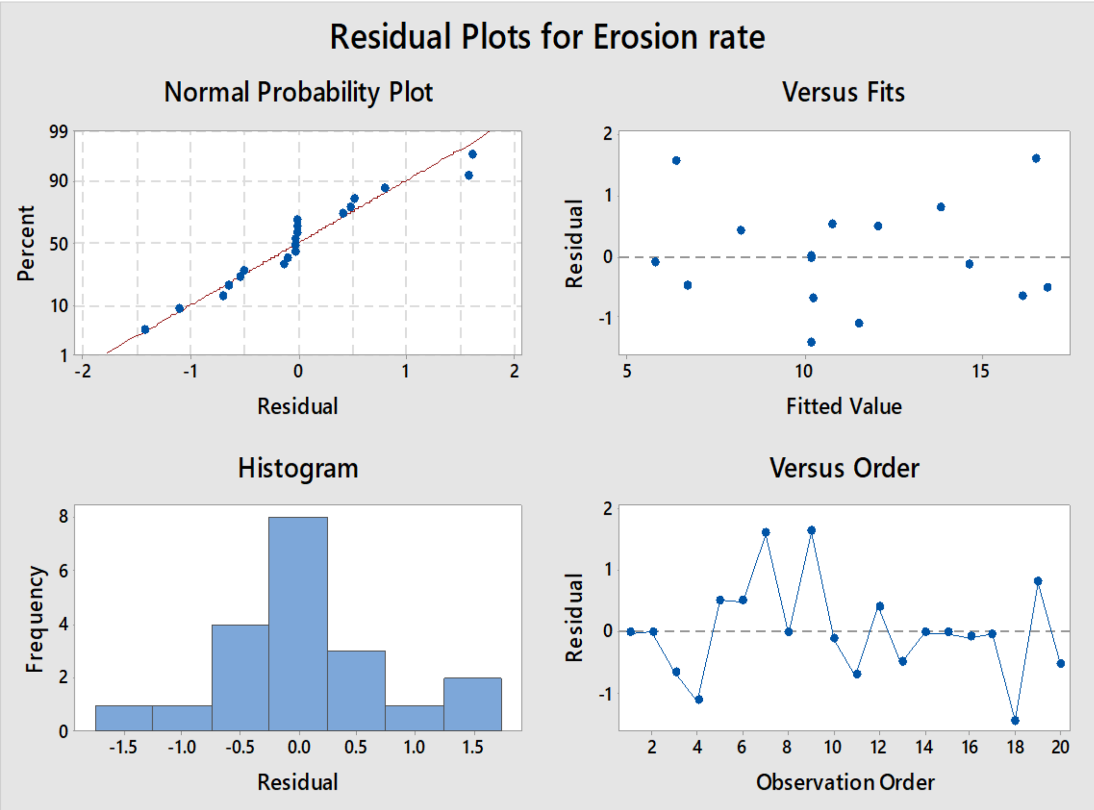

Fig. 5.2: Residual normal probability plots for Erosion rate.

Fig. 5.3 shows the 3D and 2D- surface contour plots of variation in erosion rate with the input parameter. It is observed from the contours that an increase in impact velocity, impact angle and test temperature plays a vital role. With an increase in input parameters, the material removal mechanisms like cutting and plastic deformation are more intense. Therefore, the ER is seen to increase with the increase in input parameters. Fig. 5.4 shows the SEM micrograph of the worn surface which substantiates the above statement. This micrograph shows that keeping one parameter constant, an increase in two input variables increases the width and depth of cut. Thereby, plastically deforming the materials in the form of lips. Similar behavior was reported in the chapter 4 (Sec. 4.2.1). [176].

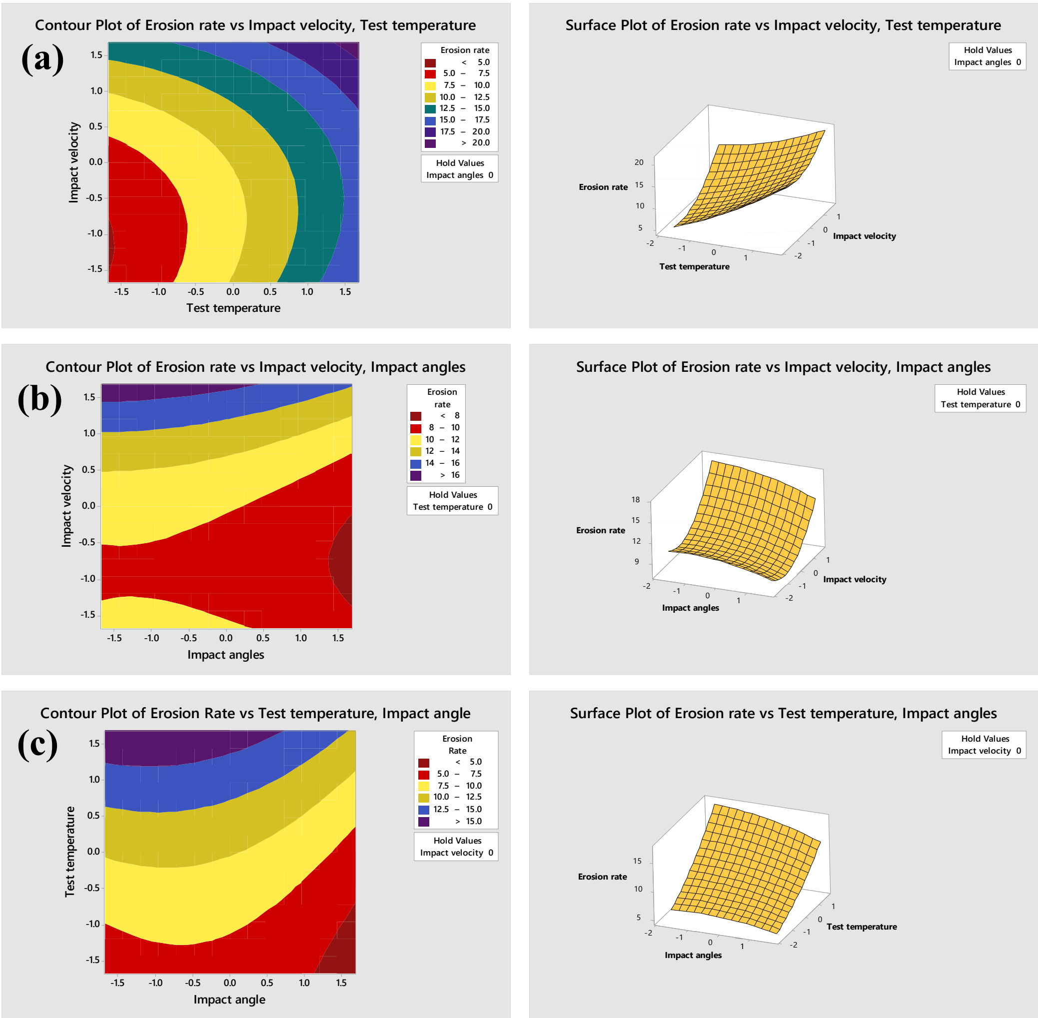

Fig 5.3: 2D-contour and 3D- surface plot showing Erosion rate variation with **(a)** test temperature-impact velocity **(b)** impact velocity-impact angle, and **(c)** test temperature-impact angle.

The average surface roughness of the worn surface was analyzed using Atomic Force Microscope (AFM). The results obtained are shown in Fig. 5.5 and the values are tabulated in Table 5.4. Here, a rougher surface with more irregularities in topography is observed as Type 446SS was eroded using higher values of "test temperature – impact velocity", shown in Fig. 5.3(a). Also, on selecting "impact velocity – impact angle", (Fig. 5.3(b)) it is observed that mild erosion rate occurs with lower values of input parameters. With further increase in impact velocity, erosion rate significantly increases for a moderate increase in impact angles. Whereas, reduction in erosion rate is recorded for higher values of both the input parameters. This indicates the occurrence of a steady state of erosive wear. This may be due to the formation of a work-hardened subsurface under the impact area.

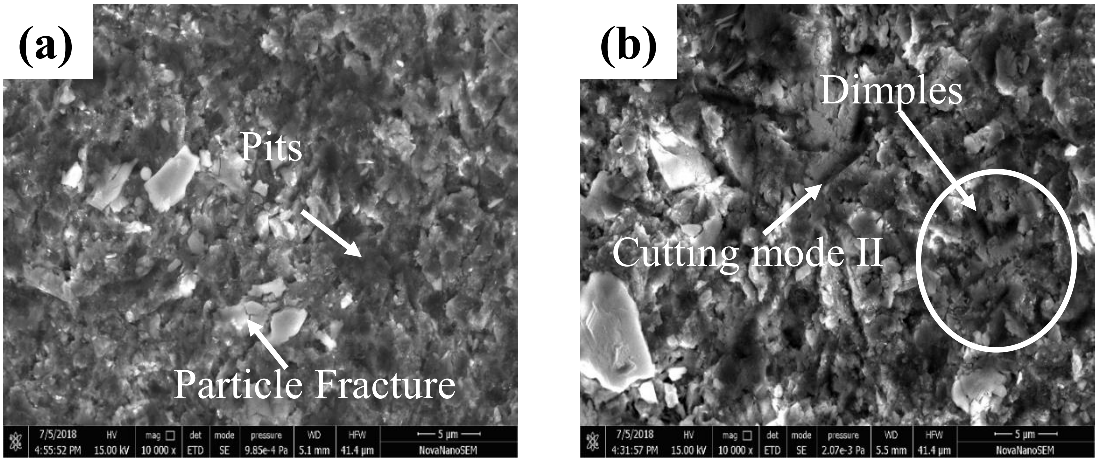

Fig. 5.4: SEM macrograph of tested sample at **(a)** 450°C, 55m/s,45° and **(b)** 650°C, 85m/s, 45°.

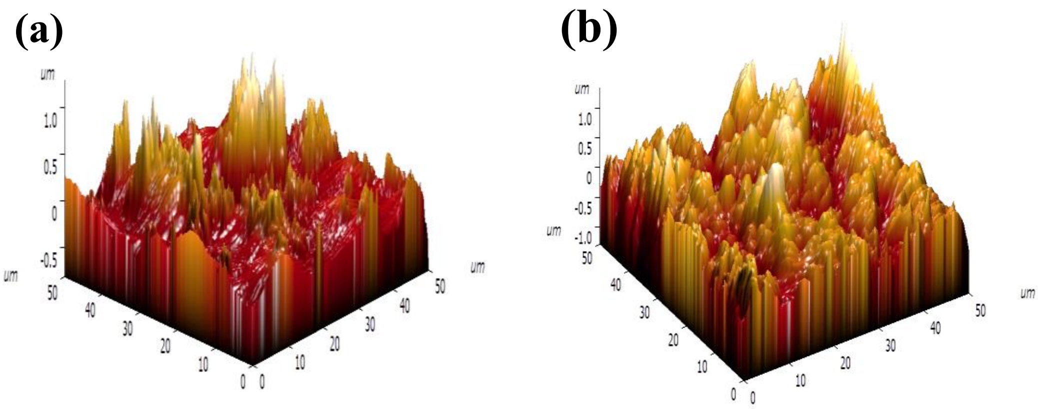

Fig. 5.5: Average Roughness (R_a) values at **(a)** 450°C, 55m/s, 45°, and **(b)** 650°C, 85m/s, 45°.

Table 5.4: Surface roughness of un-eroded and eroded surfaces.

Surface Roughness	Un-eroded	Eroded surfaces	
		450°C, 55m/s, 45°	650°C, 85m/s, 45°
Ra(μm)	0.0104	0.158	0.224

Considering the input parameters "test temperature- impact angle", the erosion rate is seen to increase with higher values of input parameters. However, beyond a certain level, with a further increase in impact angle, the erosion rate is reduced to a moderate value. This is due to the smeared surface created over a larger area during low angle impact. Still, the test temperature effect is more influencing. Main effect plot for erosion rate with test temperature, impact velocity, and impact angle is shown in Fig. 5.6.

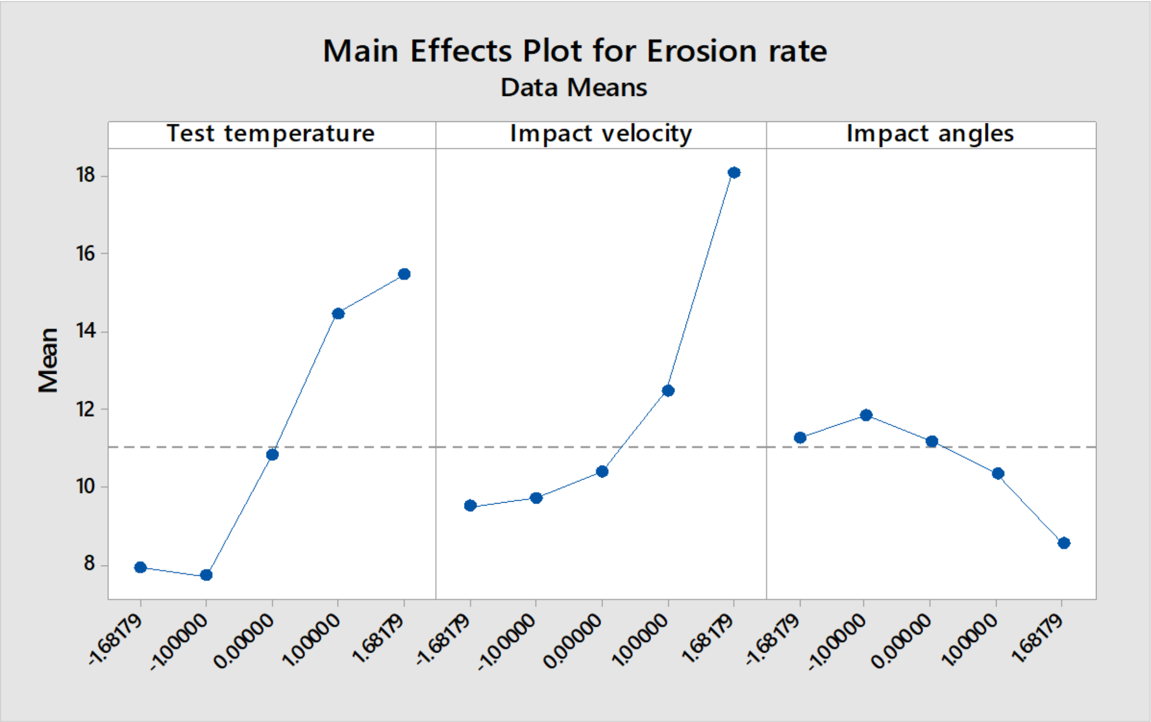

Fig. 5.6: Main effects plot for Erosion rate with test temperature, impact velocity and impact angles.

5.2.3 Prediction using artificial neural network

The database is divided into three categories, namely: (i) a validation category (ii) a training category (iii) a test Category. In the training phase, each neuron receives the input signals X_i from n neurons, assigns the weights (Wij) of the synapses to each of these inputs, according to Eq. (5.2), and passes the result as the output signal Y_i, after applying the sigmoid function, Eq. (5.3), as the transfer function.

$$Y_i = \sum_{i=1}^{n} x_i w_{ij} \tag{5.2}$$

$$f = \frac{1}{1+e^{-x}} \tag{5.3}$$

The error is minimized by adjustments of the weights according to the following mathematical equation (5.4):

$$\Delta W_{ij} = \eta \frac{\partial E}{\partial W_{ij}} \tag{5.4}$$

where η is the learning rate parameter.

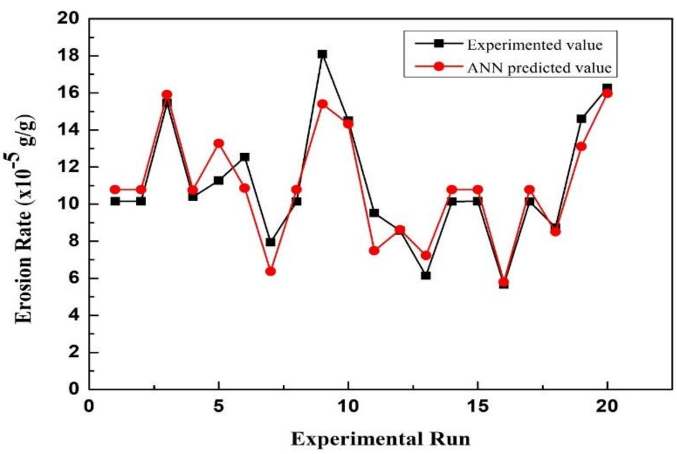

Fig. 5.7: Erosion rate comparison between ANN predicted values and experimented values.

The training parameters for the present study are listed in Table 5.5. A well trained ANN can be used to predict new results in the same knowledge domain. During the evaluation 20 data sets have been used to train the network and optimized parameters for minimum erosion obtained through RSM have been used to test the network. Fig. 5.7 shows the prediction quality of ANN structures based on mean square error.

Table 5.5: ANN training parameters.

Input parameters for training	Values
Learning parameter (η)	0.001
No. of iterations	1000000
No. of layers	3
No. of neurons in the input layer	3
No. of neurons in the hidden layer	5
No. of neurons in the output layer	1

Table 5.6 shows that error for experimented sets lies in the range of ~21%. And the error for the optimized parameter is 9.12%, as shown in Table 5.7, which establishes the validity of neural computation.

5.3 OPTIMIZATION AND VALIDATION OF THE MODEL

The aim of validating the model is fulfilled by comparing the predicted results of the model with experimental results. The optimized conditions are listed in Fig. 5.8, considering the outline erosion process to be minimized, and values for predicted and experimented results of erosion rate are tabulated in Table 5.7 and Table 5.8 respectively.

Table 5.6: Comparison of experimental and neural network output for test data set.

Experimental Run	Input (Erosion Parameters)			Output (Erosion Rate x10^{-5} g/g)		Error %
	Test temperature	Impact velocity	Impact angle	Experimental	ANN	
1	550	70	60	10.151	10.787	6.26
2	550	70	60	10.158	10.787	6.19
3	750	70	60	15.463	15.911	2.90
4	450	85	45	10.395	10.763	3.54
5	550	70	30	11.269	13.285	17.90
6	650	55	75	12.539	10.869	-13.31
7	350	70	60	7.936	6.3646	-19.81
8	550	70	60	10.148	10.787	6.29
9	550	100	60	18.095	15.407	-18.80
10	650	85	75	14.503	14.3295	-1.19
11	550	40	60	9.523	7.481	-21.44
12	550	70	90	8.573	8.623	0.58
13	450	55	45	6.140	7.2216	17.61
14	550	70	60	10.143	10.787	6.34
15	550	70	60	10.156	10.787	6.21
16	450	55	75	5.654	5.792	2.44
17	550	70	60	10.139	10.787	6.39
18	450	85	75	8.746	8.504	-2.76
19	650	55	45	14.601	13.118	-10.15
20	650	85	45	16.269	15.974	-1.81

RSM has been used to get the maximum amount of information in a short period of time and with the least number of experiments. To investigate the effect of temperature-velocity-angle, for a constant discharge, 3D response surface is plotted. These plots are useful in analyzing the interaction between parameters and to obtain their optimum condition for minimizing erosion rate. The effect of input parameters, as well as maximum and minimum points for erosion, are shown in Fig 5.3(a-c). The interaction between input parameters at low temperature, moderate velocity and high impact angle are the most optimized parameters for minimizing loss of materials.

The ANN used focuses on establishing a relationship between input and output parameters. Its evaluation capabilities are based on a comparison of predicted capabilities versus the real ones. It was important to test the neural model abilities to generalize and predict the synergistic effect of input parameters on the erosion behavior of the material. Based on neural network analysis ANN showed quite good performance in predicting the erosion rate. This network was used to work with DOE and RSM to optimize the erosion rate. The optimization is performed using Minitab Response Optimizer, and the optimum parameters that resulted in minimum erosion rate are: test temperature of 350°C, impact velocity of 55m/s and impact angle of 90°. It is observed that as the test temperature and impact velocity increases, the erosion rate also increases. However, with an increase in impact angle, the erosion rate decreases. The materials exhibit ductile behavior, therefore, results in reduced erosion at a normal impact. Three confirmatory tests are performed to check the adequacy of the predicted model with the experimented model. It is inferred that the error lies between 7.54% and 12.81%. This error is due to process incapability since the machine follows a normal distribution and therefore, replication of any experimented results follows deviation. The error is assessed as small, and therefore the model is satisfactory.

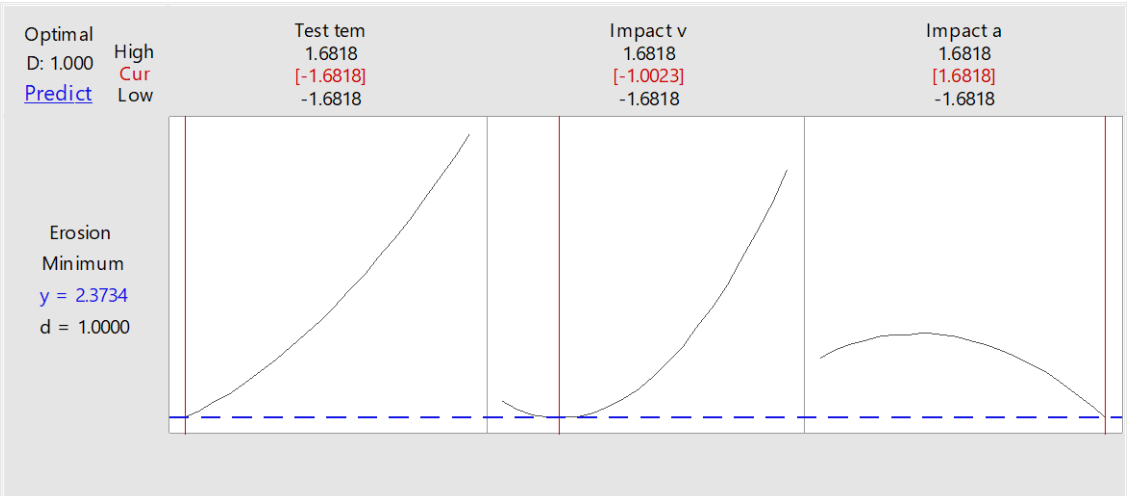

Fig. 5.8: Optimum results for minimum erosion rate.

Table 5.7: Predicted values of the model for erosion rate.

Parameters	Optimum values	Erosion rate (g/g x10^{-5})	
		CCRD values	ANN values
Test temperature	350°C	3.618	3.948
Impact velocity	55 m/s		
Impact angles	90º		

Table 5.8: Experimented values for erosion rate.

Test No.	Optimum values	Erosion rate (g/g x10^{-5})	Error (%)
1	350°C	4.081	12.81
2	55 m/s	3.891	7.54
3	90º	3.997	10.45

5.4. CONCLUSIONS

To avoid redundancy in a number of experiments and time consumption, optimization of erosion rate with variable input parameters is essential. Following are the conclusions drawn from the present study:

1. The results reveal that "test temperature" is the most dominant factor for erosion rate followed by impact velocity and impact angle.
2. The mathematical model helps in achieving the optimum parameters, of 350°C test temperature, 55 m/s impact velocity, and 90º impact angle, to achieve minimum erosion rate.
3. Conformity tests with error value between 7.54% and 12.81% indicated that the model equation is in good agreement with experimental values.
4. The results are in accordance with the established theory of maximum wear rate with oblique impact and vice-versa.
5. The artificial neural network technique was applied to predict the erosion rate of Type 446SS. The error of 9.12% in the result shows the acceptability of predicted data when compared to measured values.

